

The performance of a screw compressor with involute contact rotors in a low viscosity gas-liquid mixture environment

N. Stošić, I. K. Smith, London/GB; J. J. Brasz, V. Sishla, Syracuse/USA

Abstract

The failure of screw compressors when operating with a low viscosity liquid, such as water, as the cooling and sealing medium is usually due to either unsuitable rotor profiling or surface material properties. This paper describes the results of a test programme on a twin screw compressor in which the rotor profiles were based on a rack generation procedure. This permitted involute meshing on the contact belt with low torque transfer between the rotors, both of which features are desirable when lubrication is poor. The machine of a 5/6 configuration with a main rotor diameter of 128 mm diameter was designed and tested. It was tested first with oil injection and later, using both coated and uncoated rotors, with water injection only. No performance deterioration with time was observed in any of these cases and, in the case of water injection, after 150 hours operation with coated rotors and 5 hours with uncoated rotors, there were no signs of contact wear. However, the test results showed that the volumetric efficiency was lower and adiabatic efficiency was higher for water injection than for oil injection.

Key Words Screw compressor performance, low viscosity liquid injection, involute profile rotors

Zusammenfassung

Das Scheitern eines Schraubverdichters, der mit einer Niedrigviskositätsflüssigkeit wie das Wasser als ein Kühl- und Verdichtungsmedium arbeitet, ist entweder durch eine ungeeignete Profilierung oder durch die unzufriedenstellende Eigenschaften des oberflächlichen Materials verursacht. Dieser Artikel beschreibt die Ergebnisse eines Testprogrammes mit einem Schraubenverdichter, wobei sich die Rotorprofile auf einer Zahnstange Generation Prozedur basieren. Dies ermöglichte ein evolventes Ineinandergreifen in der Kontaktzone mit einer niedrigen Drehmomentübertragung zwischen den Rotoren, was man als sehr gewünscht betrachtet, wenn die Schmierung unzureichend ist. Die Maschine, die entworfen und konstruiert wurde, hat eine 5/6 Konfiguration mit dem Hauptrotordurchmesser von 128mm. Diese Maschine wurde zuerst mit der Öleinspritzung, und danach nur mit der Wassereinspritzung, wobei beschichtete als auch die unbeschichtete Rotoren in den Betrieb gesetzt wurden, getestet. Im Laufe des Testprogrammes wurden keine Leistungsver schlechterungen gemessen, und im Falle der Wassereinspritzung gab es nach 150 Stunden des Laufes mit den beschichteten und 5 Stunden mit den unbeschichteten Rotoren keine Zeichen der Abnutzung von Berührungsflächen. Jedoch, die Ergebnisse haben gezeigt, dass die volumetrische Leistung niedriger und die adiabatische Leistung höher für die Wassereinspritzung war als für die Öleinspritzung.

Schlußwörter: Schraubenverdichterleistung, Niedrigviskositätsflüssigkeitseinspritzung, Rotoren mit Evolventenflanken

1. Introduction

A programme for the development of scREW compressors and expanders is being carried out as reported in *Smith et al, 1996* and *Stošić et al, 1997*. In the case of machines used for two-phase fluids, the possibility of relying on the working fluid for rotor lubrication was considered since it has already been shown by *Kauder and Dämgen, 1994*, that a compressor with coated rotors could run successfully using water injection.

In the present development, the estimated characteristics of the rotor profiles were considered to make the possibility more favourable. These are shown in Fig 1. They are of a novel type which have been developed and tested here extensively. Both male and female lobes are generated from a rack which has the form of a straight line in the region of the contact band. This gives them an involute form in that area which implies that the contact between the two rotors is the best possible. A further feature of this rotor profile is that there is very little torque transmission through the female rotor and hence the contact forces between the rotors are small. They also have other advantages including a very high cross sectional flow area, strong gate rotor lobes and a clearance distribution such that in the event of hard contact between the rotors, they will not seize. Patent applications have been filed for the family of profiles thus generated, *Stošić 1996*.

As a preliminary test, it was considered to be worthwhile to evaluate the air compressor to run without timing gear using water as a coolant in order to obtain high pressure discharge without overheating. A further object of such tests was to determine the suitability of a novel coating process to enable rotors to run in contact without oil lubrication. Accordingly a programme was implemented to carry out a 150 hour endurance test on the machine using coated rotors when running at the same speed and pressure ratio as the air compressor. This was followed by a further 5 hours running under the same operating conditions but with uncoated rotors. The programme was carried out in its entirety between September 1997 and January 1998.

2. Generation of a 'Low Contact Stress' Involute profile

Twin screw compressor rotors have parallel axes and a uniform lead and they are therefore a form of helical gears. They theoretically make line contact, but contact is terminated in regions remote from the pitch circles in order to minimize the sliding component of motion between them. The conjugacy criterion in the transverse plane perpendicular to their axes is the same for helical rotors as for spur gears, i.e. it is fully defined in only one plane.

For such machines to perform effectively, the rotors must meet all the engaging requirements of helical gears and, in addition, they should maintain a seal around the entire profile. The envelope method which states that *two surfaces are conjugate if each generates or envelopes the other under a specified relative motion* may be invoked to meet the gearing requirements. Either real or hypothetical rotors may be used to define primary arcs. A convenient one is a rack, which is a rotor with infinite radius.

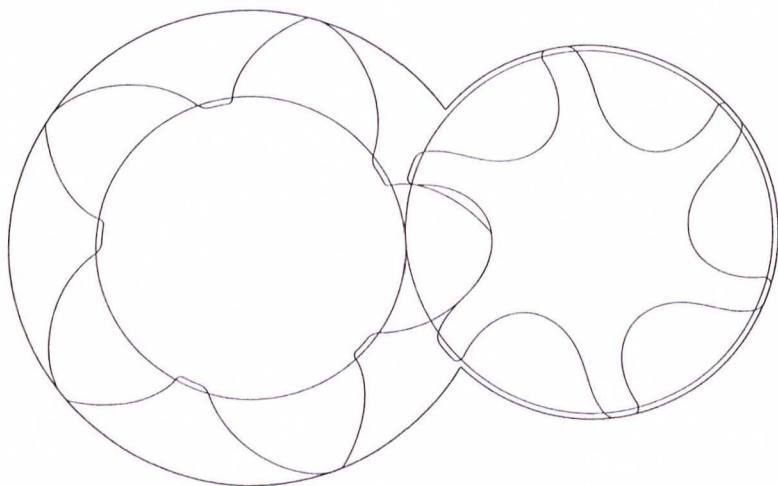


Fig. 1. "N" Profile Rotors as Used in the Screw Compressor Tests
Bild 1. "N" Rotoren benutzt in Schraubenverdichtertesten

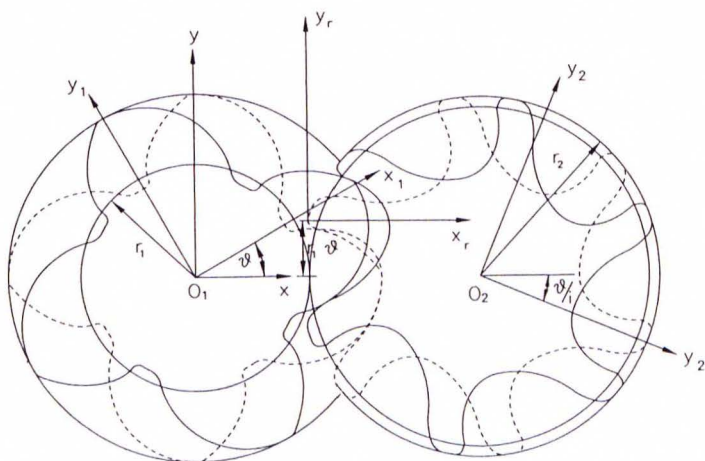


Fig. 2. Coordinate Systems of Helical Rotors
Bild 2. Koordinatensysteme der Schrägverzahnung

The rack has advantages over any other, real or imaginary type of rotor. The length of the rack profile is shorter than that of any other rotor, which means that it will be transponded to other rotors without loops during the generation. This is specially significant for rotor manufacturing. Also, a rotor generated from a rack enables involutes to be generated on the rotors from the straight lines on the rack. The involutes on both rotors enable rotor contact with the largest possible combination of radii of curvature thereby ensuring the smallest rotor contact stress. The rotor clearance distribution may be adjusted to limit the rotor contact to a shorter profile length adjacent to the pitch circles than for other rotors.

Primary arc coordinates x_r and y_r are given as arbitrary functions of a parameter t on the rack.

$$x_r = x_r(t) \quad (1)$$

$$y_r = y_r(t) \quad (2)$$

From this, the secondary arc coordinates on one of the rotors are derived as functions of both, t and θ , where θ is a position parameter. The main rotor profile coordinates x_1 and y_1 are obtained from the rack in coordinate system given in Fig. 2:

$$x_1 = x_1(t, \theta) = (x_r + r_1) \cos \theta - (y_r - r_1 \theta) \sin \theta \quad (3)$$

$$y_1 = y_1(t, \theta) = (x_r + r_1) \sin \theta + (y_r - r_1 \theta) \cos \theta \quad (4)$$

The gate rotor profile coordinates x_2 and y_2 obtained from the rack are:

$$x_2 = x_2(t, \theta) = (x_r + r_2) \cos \frac{\theta}{i} + (y_r - r_2 \frac{\theta}{i}) \sin \frac{\theta}{i} \quad (5)$$

$$y_2 = y_2(t, \theta) = -(x_r + r_2) \sin \frac{\theta}{i} + (y_r - r_2 \frac{\theta}{i}) \cos \frac{\theta}{i} \quad (6)$$

There, r_1 and r_2 are the main and gate rotor pitch circle radii respectively. θ represents the value of the rotation angle of the main rotor at which the primary arc on the rack and the secondary arc on the gate rotor have contact for each value of t . To ensure proper meshing, this angle must satisfy an envelope conjugacy condition:

$$\frac{\partial x_r}{\partial t} \frac{\partial y_r}{\partial \theta} - \frac{\partial y_r}{\partial t} \frac{\partial x_r}{\partial \theta} = 0 \quad (7)$$

The expanded form is:

$$\frac{\partial y_r}{\partial x_r} (r_1 \theta - y_r) - x_r = 0 \quad (8)$$

Once obtained, the distribution of $\theta = \theta(t)$ around the profile may be used to calculate conjugate rotor profile point coordinates as well as to determine the sealing, or contact lines and paths between the two rotors.

Rinder, 1984 used a similar procedure to generate his involute rotors.

More details on the application of the envelope method to screw compressor rotor gearing may be found in *Stosić 1998*.

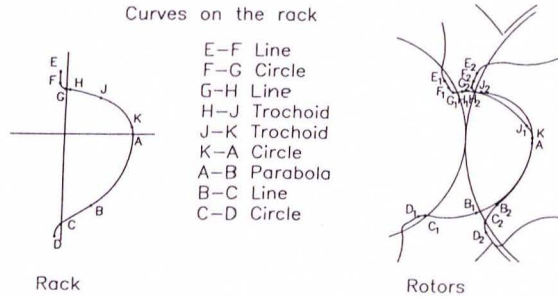


Fig. 3. "N" Rack and Rotor Profile Key Points
Bild 3. Die Hauptpunkte der "N" Zahnstange und Rotorenprofile

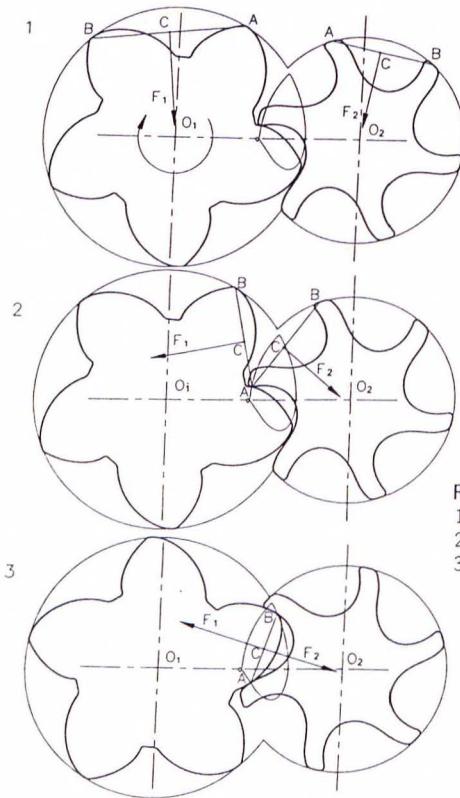


Fig. 4.

Radial Forces and Torque:

1. No contact points
2. Interlobe contact at one point,
3. Interlobe contact at two points

Bild 4.

Radialkräfte und Drehmoment:

1. Keine Berührungspunkte,
2. Die Berührung in einem Punkt,
3. Die Berührung in zwei Punkten

The following is a brief description of a rotor profile, typical of a whole family, designed for the efficient compression of air, common refrigerants and a number of process gases, in which there is special emphasis on obtaining low contact stress between the rotors. The aim is reached by combining the optimal involute rotor contact and low contact force.

The coordinates of all primary arcs are defined on the rack and summarized here relative to the rack coordinate system. The division between the profile arcs is denoted by capital letters and each arc is defined separately, as shown in Fig. 3 where the rotor rack and rotors are shown together. More details are given in *Stošić and Hanjajić, 1997*.

Segment $E - F$ is a straight line and $F - G$ is a circular arc. $G - H$ is a straight line which forms the upper involute. To minimize the blow-hole area, segment $H - J$ on the rack is cut as a trochoid generated by the small portion of the arc $H_2 - J_2$ on the gate rotor, while segment $J - A$ on the rack is another trochoid generated by the small portion of the arc $A_1 - J_1$ on the main rotor. $K - A$ is a circular arc while segment $A - B$ is a parabolic arc on the rack. This ensures both a large rotor displacement and a low torque on the gate rotor. $B - C$ is a straight line on the rack which is required for the lower involute, while $C - D$ is a circular arc on the rack. Segment $D - E$ is a straight line on the rack which completes parts of the rotor inner/outer circles.

A variety of profiles can be generated from this template. The profile design is a compromise between *i*) full tightness, *ii*) small blow-hole area, *iii*) large displacement, *iv*) short sealing lines, *v*) small confined volumes, *vi*) involute rotor contact and *vii*) proper gate rotor torque distribution together with *viii*) high rotor mechanical rigidity. The blow-hole area may be controlled by adjustment of the tip radii on both the main and gate rotors and also by making the gate outer diameter equal to or less than the pitch diameter. Rotor instability, which is often caused by inappropriate torque distribution in the gate rotor may be avoided by tuning the exponent of the rotor parabola. Furthermore, full involute contact between the "N" rotors enables any additional contact load to be absorbed more easily than by other types of rotors.

3. Contact Forces on Screw Compressor Rotors

Screw compressor rotors are subjected to severe pressure loads. The rotors, as well as the rotor bearings must satisfy rigidity and elasticity requirements to ensure appropriate and reliable compressor operation. The contact force between the rotors, which is determined by the torque transferred between rotors, plays a key role in compressors with direct rotor contact. The contact force is small in the case of a main rotor driven compressor. In the case of a gate rotor drive, the contact force is substantially larger. Therefore this latter case is excluded from any serious consideration for low viscosity fluid flooding.

A mathematical model, represented by a set of equations which describe the physics of the complete process in a compressor is used to calculate the contact forces acting between the compressor rotors. The equation set consists of the conservation equations for energy and mass as well as the momentum equation supported by a number of algebraic equations

defining leakage and fluid injection and other accompanying phenomena.

The solution of the equation set is performed numerically by employing the Runge-Kutta 4th order method, with appropriate initial and boundary conditions for the fluid suction, compression and discharge. As a result, the trapped mass, pressure and temperature in the working chamber is calculated as a function of the rotation angle θ . These are then used in further calculations on the $p-V$ diagram to obtain compressor power, compressor fluid flow and oil flow, turbulence and heat transfer. Finally, the specific power, volumetric and adiabatic efficiencies are calculated to give complete information of the compressor process. For example, p is then used for calculations of the rotor contact forces. More details of the modelling procedure are given in *Hanjalić and Stošić, 1997*.

The calculation procedure of pressure loads follows *Rinder 1979*. The pressure $p = p(\varphi)$ function is known for any instantaneous angle of rotation φ , with a reasonable angle increment. Fig. 4 presents the radial and circumferential forces in a rotor cross section. A pressure p acts in the corresponding interlobes normal to line AB . A and B are either on the sealing line between the rotors or on the rotor tips. They are fully defined from the rotor geometry.

In position 1, there is no contact between the rotors, since A and B are on the circle and overall forces F_1 and F_2 act towards the rotor axes. There is no torque caused by pressure forces in this position. In the next position there is only one contact point between the rotors; point A . Forces F_1 and F_2 are eccentric, they comprise the radial and circumferential components. The latter cause the torque. In the case of a main driven rotor, the torque on the gate rotor, which is significantly smaller than the main rotor torque, defines the contact force. In position 3, both contact points are on the rotors and the overall and radial forces are equal for both rotors but there still is a torque between the rotors.

The torque which defines the contact force between rotors is:

$$T = p \int_A^B x dx + p \int_A^B y dy = 0.5p(x_B^2 - x_A^2 + y_B^2 - y_A^2) \quad (9)$$

A and B are on the sealing line. The above equation is integrated around the profile for all profile points. Then it is integrated for all angle steps to complete one revolution employing a given pressure history. Finally, the sum is made for all rotor interlobes, taking into account the phase shift as well as the axial shift between the interlobes.

The calculation results are presented in Fig. 5 in the form of a torque-angle diagram. As may be noted, the torque between the two rotors caused by pressure, is low but is always positive. This means that contact between the two rotors will be on one side of the rotors only.

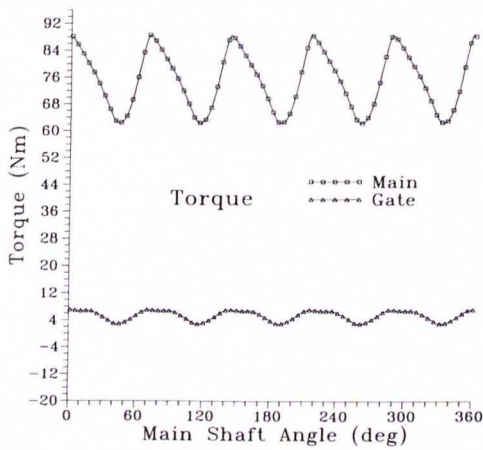


Fig. 5. Main and Gate Rotor Torque Distribution in one Compressor Revolution
Bild 5. Haupt- und Nebenläuferdrehmomentverteilung in einer Kompressorumdrehung

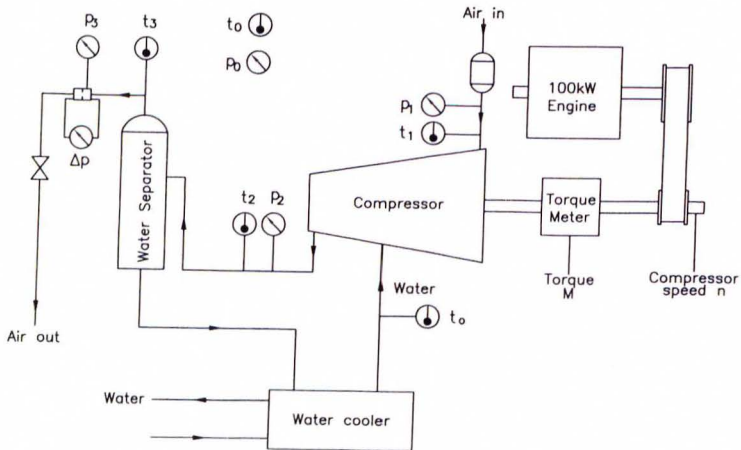


Fig. 6. Layout of Air Compressor test Rig as Modified for Operation with Water Injection
Bild 6. Die Anordnung eines für den Betrieb mit der Wassereinspritzung modifizierten Luftkompressorexperimentstandes

4. Machine Design and Manufacture

For test purposes four pairs of rotors were manufactured and paired by a specialist rotor manufacturer. Two of these pairs were coated while the other two were left in the finished metal state.

To obtain the best performance from compressors with advanced rotor profiles it is essential that all other components are designed to take advantage of the benefits which the rotors confer. Special care was given to minimise the flow losses in the suction and discharge ports. The low pressure port was positioned in the housing to let the air enter with the fewest possible bends and the air approach velocity was kept low by making the flow area as large as possible. The high pressure port size was first determined by estimating the built-in-volume ratio required for optimum thermodynamic performance. It was then increased in order to reduce the exit air velocity and hence obtain the minimum combination of internal and discharge flow losses.

The cast iron casing, which was carefully dimensioned to minimize its weight, contained a reinforcing bar across the suction port to improve its rigidity at higher pressures.

5. Compressor Performance Measurements

5.1 The Test Rig

A test rig has been designed and constructed at the City University Compressor Centre Laboratory and certified by Lloyd's Register as meeting Pneuop/Cagi requirements for air compressor acceptance tests. High accuracy test equipment is used for the measurement of all relevant parameters. All measurements are made by transducers and are recorded and processed in a data logger. Due to the large electrical power requirements of the engine laboratory in which the test facility is located, a 100 kW turbo charged intercooled diesel engine is used as the power source to drive the compressor which is connected to the compressor test bed by a vee belt drive with a 2.5:1 ratio speed step up. This may operate at variable speed to test liquid-flooded air compressors with discharge rates of up to $16 \text{ m}^3/\text{min}$.

This test rig was developed primarily for the testing of oil injected twin screw air compressors. The compressor may be connected to either end of the drive shaft, which is mounted in plummer blocks, in order to eliminate side loads in the final drive. This arrangement thus allows for compressor rotation in either direction.

A major component of the test assembly is the oil separator which is built in two stages. Oil separated from the discharged air at high pressure is reinjected into the compressor through the oil injection jet within the main compressor casing. Drillings within the compressor body also lead some of the reinjected oil to lubricate the compressor bearings. For the purpose of these tests, the oil separator was converted to a water separator and store. The oil injection jet and internal oil circulation drillings in the compressor were

blanked off and all the water injected was admitted directly through the inlet port of the compressor together with the air. In addition provision had to be made to recover water which leaked into the bearing housings and pump it back to the air inlet port. In order to minimise corrosion, the injected water contained 20% of ethylene glycol. A diagram of the modified rig and relevant measurements taken are shown in Fig 6. The following parameters are measured directly.

p_0	- Atmospheric pressure [mmHg]	t_1	- Suction temperature [°C]
p_1	- Suction pressure [b]	t_2	- Discharge temperature [°C]
p_2	- Discharge pressure [b]	t_3	- Orifice plate temperature [°C]
p_3	- Orifice plate pressure [b]	t_3	- Water injection temp. [°C]
Δp	- Orifice plate pressure difference [Pa]	M	- Torque [Nm]
n	- Compressor speed [rpm]		

5.2 The Test Programme

The requirements for the complete test programme were as follows:

- i) Obtain a set of samples of the coated rotor surface.
- ii) Install the coated rotors in the compressor and run at 3600 rpm and a power input of 30 kW corresponding to a discharge pressure of 7 bar, to carry out: a) A 5 hour initial test run followed by a partial strip down and inspection of the rotors and obtaining a second set of rotor surface samples. b) A further 145 hours operation followed by a strip down and further inspection of the rotors and the taking of a final set of samples from the coated rotor surfaces.
- iii) Rebuild the compressor with plain metal rotors and run for a further 5 hours at 3600 rpm and 7 bar discharge pressure.

The initial running of the compressor was carried out after a set of samples of the coated rotor surface was obtained and rotors washed with acetone. Soon after start up it was found that water was leaking into the lubricating oil. It was therefore decided to shut down after 90 minutes running to replace the oil lubrication system with grease. At the same time, the rotors were inspected and further surface samples were taken.

Testing was then resumed and the compressor was run for a further 123.5 hours. At this time the compressor failed to start up at the beginning of the day's run. Inspection revealed that the inner track of the outer ring of the female rotor discharge bearing was heavily worn. It was thought to be due to corrosion caused by ingress of water into the grease packed bearing. The bearing was replaced and the remaining 25 hours running time was then completed successfully.

The rotors were then inspected again and samples were taken of their surfaces. Rotor wear appeared to be negligible with only a light polish on the contact bands of each rotor. This is shown in Fig. 7. The inner track of the outer ring of the female rotor discharge bearing was examined and found to have worn in a similar manner to the one it had

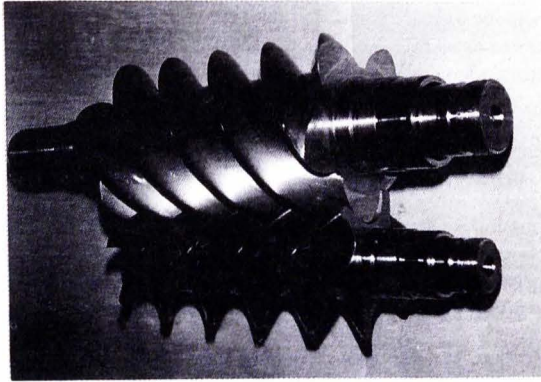


Fig. 7. View of the Rotors after 150 Hours Running Time
Bild 7. Die Ansicht des Rotoren nach 150 Arbeitsstunden

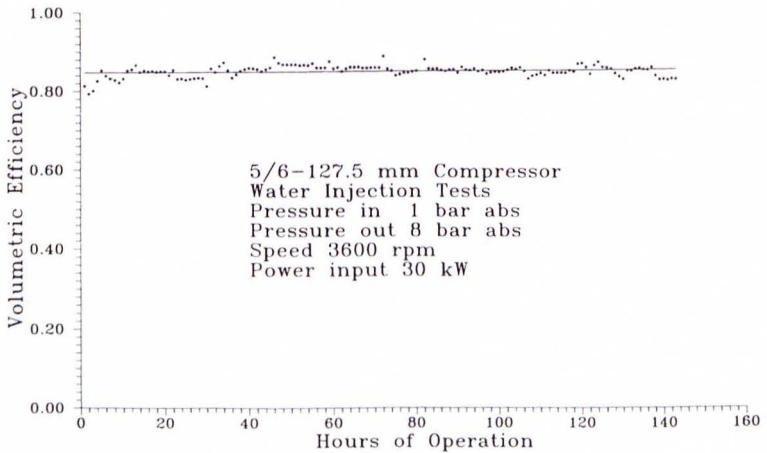


Fig. 8. Variation of Volumetric Efficiency over the Test Period
Bild 8. Die Variation der volumetrischen Leistung im Ablauf des Experimentes

replaced but not so heavily. Further inspection then revealed that the failure was not due to corrosion but rather to loose fitting of the outer bearing race in the compressor casing. This had caused fretting action which led to the first bearing failure.

The compressor was then reassembled with uncoated rotors and run for a further 5 hours without failure. On completion of the final five hours operation, the rotors were inspected and found to be only lightly polished along their contact belts.

Apart from the bearing failure reported, which was due to acceptance of the casing with the bearing housing bore over the maximum allowed tolerance, the compressor ran well with almost no variation in speed, discharge pressure, applied torque and air discharge and bearing temperatures over prolonged running periods of up to 12 hours per day.

Due to the water injection, the temperature rise of the compressed air was only of the order of 8°C while the water temperature, which was much cooler on admission, rose by approximately 17°C . Because of this near isothermal compression of the air, the compressor operated with an exceptionally high adiabatic efficiency, despite that fact that its built in volume ratio was too small for the required discharge pressure.

Another feature of the water injection was that due to the very low temperature rise of the air, the amount of water vapour which could be carried off by evaporation into the air, was very small and amounted to little more than 15 litres over the entire test programme.

A problem which occurred as a result of running with water injection was that, even with added ethylene glycol, the compressor casing tended to rust when left static. To prevent this when the compressor was switched off at night, warm air from a fan heater was directed over the compressor to rise its temperature at approximately 80°C and dry it.

5.3 Test Results

Log sheets were maintained for the entire test programme. Performance analyses were carried out on the test data and the results of these are shown in Figs 8-10. As may be deduced from them, the the average adiabatic and volumetric efficiencies of the compressor during operation were 94% and 88% respectively while the specific power input was approximately $5.9\text{ kW/m}^3/\text{min}$. The high adiabatic efficiency is, of course, due to the exceptional cooling effects of the water but the volumetric efficiency is somewhat lower than normally obtained for a machine of this type using oil injection. It is believed that this is due to the water having a much lower viscosity and hence not sealing the clearance gaps so effectively. The specific power input is slightly higher than obtained for a similar machine run as an oil flooded compressor. This is due to the reduced volumetric efficiency. Otherwise, with such a high adiabatic efficiency, it would have been significantly lower.

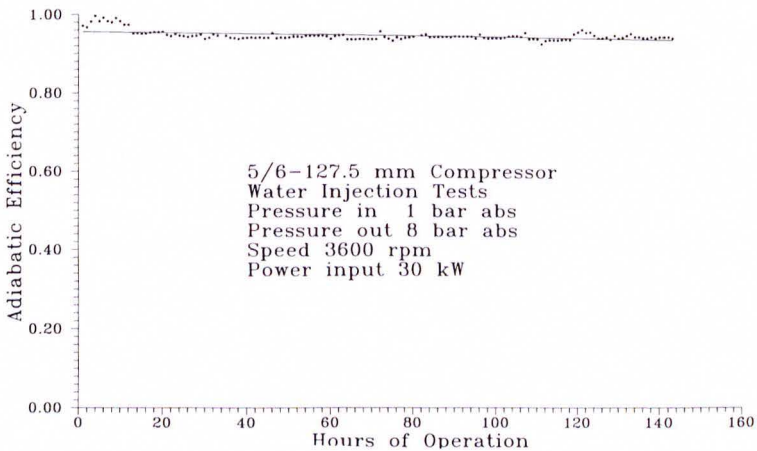


Fig. 9. Variation of Adiabatic Efficiency over the Test Period

Bild 9. Die Variation der adiabatischen Leistung im Ablauf des Experimentes

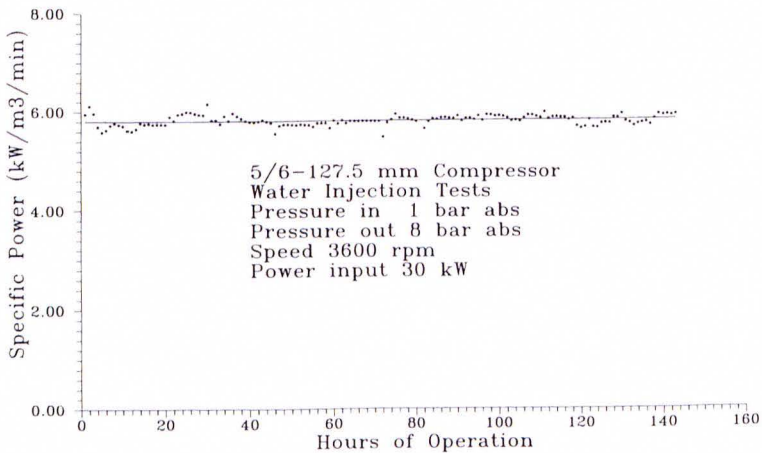


Fig. 10. Variation of Specific Power Input over the Test Period

Bild 10. Die Variation der spezifischen Leistung im Ablauf des Experimentes

6. Conclusions

The method of screw rotor profile generation used by the authors for a long time to generate screw rotor profiles has been demonstrated. It is convenient both for the design of new rotors and the improvement of existing designs. The mathematically rigorous method used has the additional advantage of simplicity which enables a variety of profiles be created in a short time by almost all mechanical engineering designers, whereas at present, such skills are known to only a limited number of exclusive specialists.

Coated rotors showed excellent wear characteristics after 150 hours running time. The condition of the uncoated rotors at the end of 5 hours operation was very encouraging

References

1. *Hanjalić K, Stojić N, 1997: Development and Optimization of Screw Machines with a Simulation Model, Part II: Thermodynamic Performance Simulation and Design, ASME Transactions, Journal of Fluids Engineering, Vol 119, p 664*
2. *Kauder K. and Dämgen U, 1994: Wasserspritzung in Schraubenkompressoren (Water Injection into Screw Compressors) "Schraubenmaschinen 94" VDI Berichte Nr. 1135 Düsseldorf*
3. *Litvin F.L, 1956: Teoria zubchatih zaceplenii (Theory of Gearing), Nauka Moscow, also second edition 1968, also NASA Ref. Publ. 212 AVSCOM Techn. report 88- C-035 1990*
4. *Rinder L, 1979: Schraubenverdichter (Screw Compressors), Springer Verlag, New York*
5. *Rinder L, 1984: Schraubenverdichterläufer mit Evolventenflanken (Screw Compressor Rotor with Involute Lobes), Proc. VDI Tagung "Schraubenmaschinen 84" VDI Berichte Nr. 521 Düsseldorf*
6. *Sakun I.A, 1960: Vintovie kompresorii (Screw Compressors), Mashinostroenie Leningrad*
7. *Smith I. K, Stojić N, Aldis C. A, 1996: Development of the trilateral flash cycle system, Part 3: the design of high efficiency two-phase screw expanders, Proceedings of IMechEng, Journal of Power and Energy, Vol 210, p 75*
8. *Stojić N, 1996: Patent Application GB 9610289.2*
9. *Stojić N, Hanjalić K, 1997: Development and Optimization of Screw Machines with a Simulation Model, Part I: Profile Generation, ASME Transactions, Journal of Fluids Engineering, Vol 119, p 659*
10. *Stojić N, Smith I. K, Kovačević A, Aldis C. A, 1997: The Design of a Twin-screw Compressor Based on a New Profile, Journal of Engineering Design, Vol 8, p 389*
11. *Stojić N, 1998: On Gearing of Helical Screw Compressor Rotors, Proceedings of IMechEng, Journal of Mechanical Engineering Science, accepted for publication, 1998*